3900 *Chem. Mater.* **2010,** *22,* 3900–3908
DOI:10.1021/cm9037846

CHEMISTRY OF MATERIALS
Article

Synthesis of Mesoporous Silica Nanospheres Promoted by Basic Amino Acids and their Catalytic Application

Toshiyuki Yokoi, Takumi Karouji, Seigo Ohta, Junko N. Kondo, and Takashi Tatsumi*

Chemical Resources Laboratory, Tokyo Institute of Technology, 4259 Nagatsuta, Midori-ku, Yokohama 226-8503, Japan

Received December 17, 2009. Revised Manuscript Received May 11, 2010

Discrete mesoporous silica nanospheres (MSNSs) with a narrow size distribution were prepared by a newly developed method, which is based on the emulsion system containing $Si(OEt)_4$ (TEOS), water, cationic surfactant, and basic amino acid under weakly basic conditions (pH 9−10). The average 20 nm sized discrete MSNSs have uniform craterlike mesopores about 3 nm in diameter. The size of the discrete spheres can be regulated in the range of 15−200 nm by, for example, changing the stirring rate in the synthesis stage. Furthermore, introduction of tetrahedrally coordinated Ti species onto the pore of MSNSs and their catalytic performance in epoxidation of different-sized alkenes, cyclohexene, *cis*-stilbene and caryophyllene were also demonstrated.

1. Introduction

Mesoporous materials with size-tunable mesopores have attracted a great deal of attention because of their controllable structures and compositions, which make them suitable for a wide range of applications in catalysis, adsorption, separation, chromatography, etc.[1] Among diverse studies on mesoporous materials, morphological control of the particle is an important issue in terms of mass transport.[2] The spherical mesoporous silica particles have been synthesized by modifying the Stöber method, which is based on the TEOS/ammonia/water/alcohol system for producing monodispersed silica spheres;[3] 0.1−2 μm sized spherical mesoporous silica particles have been obtained under diluted surfactant concentration to hinder the particle aggregation.[4,5] However, the size of the particles was not highly uniform, and the yield of the silica was low. Up to now, intensive and extensive studies have been conducted on the preparation of nanometer-sized mesoporous silica particles.[6−11] For example, Mann et al. succeeded in fabricating nanoparticles with mesostructured interiors through a quenching procedure in the template-directed synthesis of MCM-41.[12] Imai et al. established a method of preparing ca. 20 nm-sized silica nanoparticles having mesopores with a uniform aperture of ca. 2 nm by using a nonionic surfactant as a suppressant of grain growth.[13] Bein et al. reported the preparation of colloidal suspensions of nanometer-sized mesoporous silica by using triethanolamine in place of conventional base sources.[14,15] Recently, Kuroda et al. succeeded in the preparation of hierarchically porous materials by assembling mesoporous nanoparticles via a spray drying route.[16] Shi et al. reported the size-controlled synthesis of monodispersed mesoporous silica nanospheres in the cosurfactant/cosolvent system.[17] Most recently, Huo et al. also reported synthesis of mesoporous silica nanoparticles via controlled hydrolysis and condensation of silicon alkoxide.[18] However, these methods are not simple but rather complicated, and the control of nanometer-scale and morphology of the particle has not been sufficiently achieved.

*Corresponding author. Phone: +81-45-924-5238. Fax: +81-45-924-5282. E-mail: ttatsumi@cat.res.titech.ac.jp.

(1) These efforts have been excellently summarized in recent reviews, e.g.: Ying, J. Y.; Mehnert, C. P.; Wong, M. S. *Angew. Chem., Int. Ed.* **1999**, *38*, 56–77. Stein, A.; Melde, B. J.; Schroden, R. C. *Adv. Mater.* **2000**, *12*, 1403–1419. He, X.; Antonelli, D. *Angew. Chem., Int. Ed.* **2002**, *41*, 214–229. Trong, On D.; Desplantier-Giscard, D.; Danumah, C.; Kaliaguine, S. *Appl. Catal.* **2003**, *253*, 545–602. Hoffmann, F.; Cornelius, M. S.; Morell, M. J.; Fröba, M. *Angew. Chem., Int. Ed.* **2006**, *45*, 3216–3251.
(2) Rolison, D. R. *Science* **2003**, *299*, 1698–1701.
(3) Stöber, W.; Fink, A. *J. Colloid Interface Sci.* **1968**, *26*, 62–69.
(4) Grün, M.; Lauer, I.; Unger, K. K. *Adv. Mater.* **1997**, *9*, 254–257.
(5) Unger, K. K.; Kumar, D.; Grün, M.; Büchel, G.; Lüdtke, S.; Adam, T.; Schumacher, K.; Renker, S. *J. Chromatogr., A* **2000**, *892*, 47–55.
(6) Lu, Y.; Fan, H.; Stump, A.; Ward, T. L.; Rieker, T.; Brinker, C. J. *Nature* **1999**, *398*, 223–226.
(7) Cai, Q.; Luo, Z.-S.; Pang, W.-Q.; Fan, Y.-W.; Chen, X.-H.; Cui, F.-Z. *Chem. Mater.* **2001**, *13*, 258–263.
(8) Nooney, R. I.; Thirunavukkarasu, D.; Chen, Y.; Josephs, R.; Ostafin, A. E. *Chem. Mater.* **2002**, *14*, 4721–4728.
(9) Lin, H.-P.; Tsai, C.-P. *Chem. Lett.* **2003**, 1092–1093.
(10) Rathousky, J.; Zukalova, M.; Kooyman, P. J.; Zukal, A. *Colloids Surf., A* **2004**, *241*, 81–86.
(11) Chao, M.-C.; Lin, H.-P.; Mou, C.-Y. *Chem. Lett.* **2004**, *33*, 672–673.
(12) Fowler, C. E.; Khushalani, D.; Lebeau, B.; Mann, S. *Adv. Mater.* **2001**, *13*, 649–652.
(13) Suzuki, K.; Ikari, K.; Imai, H. *J. Am. Chem. Soc.* **2004**, *126*, 462–463.
(14) Möller, K.; Kobler, J.; Bein, T. *Adv. Funct. Mater.* **2007**, *17*, 605–612.
(15) Kecht, J.; Schlossbauer, A.; Bein, T. *Chem. Mater.* **2008**, *20*, 7207–7214.
(16) Urata, C.; Yamauchi, Y.; Aoyama, Y.; Imasu, J.; Todoroki, S.; Sakka, Y.; Inoue, S.; Kuroda, K. *J. Nanosci. Nanotechnol.* **2008**, *8*, 3101–3105.
(17) He, Q.; Cui, X.; Cui, F.; Guo, L.; Shi, J. *Microporous Mesoporous Mater.* **2009**, *117*, 609–616.
(18) Qiao, Z.-A.; Zhang, L.; Guo, M.; Liu, Y.; Huo, Q. *Chem. Mater.* **2009**, *21*, 3823–3829.

Published on Web 06/08/2010

We have developed a novel and simple liquid-phase method for forming uniform-sized silica nanospheres (SNSs) about 10 nm in size.[19] The SNSs can be synthesized through hydrolysis and condensation reactions of TEOS in the emulsion system containing TEOS, water, and basic amino acids under weakly basic conditions (pH 9−10). Furthermore, the size of SNSs can be tuned ranging from 8 to 35 nm by varying the compositions of the reactants.[20]

Here we report the synthesis of 15−200 nm sized discrete mesoporous silica nanospheres (MSNSs). Our strategy for preparing MSNSs is an addition of a surfactant into the system for the synthesis of SNSs mentioned above; hydrolysis and condensation reactions of TEOS were conducted in the emulsion system containing TEOS, water, basic amino acids, and cationic surfactants under weakly basic conditions (pH 9−10), not in the homogeneous system. The mechanism of the formation of MSNSs promoted by basic amino acids was proposed. Finally, preparation of Ti-containing MSNSs (Ti-MSNSs) and their catalytic performance were demonstrated.

2. Experimental Section

2.1. Chemicals. Tetraethyl orthosilicate (TEOS), tetra-*n*-butoxy orthotitanate (TBOT) and typical cationic surfactant such as hexadecyltrimethylammonium chloride (C_{16}TMACl) were purchased from Tokyo Chemical Industry. Reagent-grade basic amino acids arginine (Arg), lysine (Lys), and histidine (His) and *tert*-butyl hydroperoxide were purchased from Aldrich. Organic regents used in the catalytic reaction were purchased from Tokyo Chemical Industry, Aldrich, and Wako. All of the reagents were used as-received, without further purification.

2.2. Preparation of Mesoporous Silica Nanospheres. In a typical synthesis, C_{16}TMACl and Arg were dissolved in water with vigorous stirring at ambient temperature, followed by addition of TEOS. The molar composition of the reactants was 1:0.13:0.04:600 TEOS:C_{16}TMACl:Arg:H_2O. Note that this system consists of two phases at the beginning; one is the water phase containing Arg and C_{16}TMACl (pH: 9.7), and the other is the oil phase consisting of unhydrolyzed TEOS. The resultant solution was stirred at 500 rpm at 333 K for 24 h. After these reaction processes, no silica precipitate was observed; silica products were highly dispersed. The as-synthesized silica product was collected by evaporation of the solvents. The organic molecules such as C_{16}TMACl and Arg were removed from the as-synthesized product by either calcination in air at 823 K for 10 h or extraction using 100 mL of EtOH containing 5.2 g of ∼35 wt % HCl aq. at ambient temperature for 24 h, leading to the formation of the mesoporous silica nanospheres (MSNSs). As mentioned below, the effects of the molar compositions of the reactants and the stirring rate were investigated.

For catalytic application of MSNSs, Ti species were introduced onto the pore of MSNSs via a post-treatment method; the HCl-treated sample (1 g) was stirred in a mixture of EtOH (2.5 mL), TBOT (0.03 mmol), H_2O_2 (4.1 mmol), and H_2O (14 mmol) at ambient temperature for 24 h. The sample was collected by centrifugation, washed with EtOH, dried at 373 K, and finally calcined at 823 K for 10 h (Ti-MSNSs).

2.3. Catalytic Reaction. To verify the difference in the catalytic performance depending on the particle size, the liquid-phase epoxidation of different-sized alkenes, cyclohexene, *cis*-stilbene and caryophyllene with *tert*-butyl hydroperoxide (TBHP, 5.5 M in decane) was carried out in a round-bottom flask. In a typical run, 10 mmol of a substrate, 10 mmol of TBHP as an oxidant and 25 mg of a catalyst were mixed in the flask and heated to 303 K under vigorous stirring. The products were analyzed on a Shimadzu GC-14B gas chromatograph equipped with a 50 m OV-1 capillary column and a flame ionization detector.

2.4. Characterizations. The structures of the synthesized samples were characterized by X-ray diffraction (XRD). XRD patterns were recorded on a Rigaku Ultima III instrument equipped with a Cu Kα X-ray source (40 kV and 20 mA). Nitrogen adsorption−desorption measurements were conducted to obtain information on the mesoporosity. The measurements were conducted at 77 K on a Belsorp Mini, Bel Japan. The BET (Brunauer−Emmett−Teller) specific surface area (A_{BET}) was calculated from the adsorption data in the relative pressure ranging from 0.04 to 0.1. The pore size (D_p) distribution was calculated from the adsorption branch of isotherms using the BJH formula. Field-emission scanning electron microscope (FE-SEM) and scanning transmission electron microscope (STEM) images were obtained on a Hitachi S-5200 microscope. Transmission electron microscope (TEM) images were obtained on a JEOL JEM-2010F microscope. The samples for FE-SEM and TEM observations were observed without any metal coating. Solid-state $^1H-^{13}C$ CP/MAS NMR and ^{29}Si MAS NMR spectra were recorded on a JEOL-ECA400 spectrometer at 100.6 and 79.4 MHz and sample spinning frequencies of 4 and 5 kHz, respectively. Elemental analyses of the samples (Si/Ti ratio) were performed on an inductively coupled plasma-atomic emission spectrometer (Shimadzu ICPE-9000 spectrometer). UV−vis diffuse reflectance spectra were recorded on a V-650DS spectrometer (JASCO). The diffuse reflectance spectra were converted into the absorption spectra using the Kubelka−Munk function.

3. Results and Discussion

3.1. Characterizations of Mesoporous Silica Nanospheres (MSNSs). Figure 1a shows the typical FE-SEM image of the product after calcination, exhibiting the discrete spherical particles. By counting 200 spheres through FE-SEM observations, its mean diameter is found to be 20 nm although the size is distributed over the range of 15−25 nm. Note that craters about 3 nm in diameter are clearly observed in each spherical particle. TEM image also reveals that each spherical particle has carters about 3 nm in diameter and depth (Figure 1b). Hence, the porosity of MSNSs is attributed to craters on the sphere, not typical cylindrical pores. Such a unique porous structure in the controlled spherical morphology is unprecedented.

Figure 2 shows the XRD patterns of the products before and after calcination. One shoulder peak at $2\theta = 1.4°$ is observed in the pattern of the product before calcination. This peak is slightly shifted to a higher position ($2\theta = 1.7°$) after calcination due to the further

(19) (a) Yokoi, T.; Sakamoto, Y; Terasaki, O.; Kubota, Y.; Okubo, T.; Tatsumi, T. *J. Am. Chem. Soc.* **2006**, *128*, 13664–13665. (b) Yokoi, T.; Iwama, M.; Watanabe, R.; Sakamoto, Y.; Terasaki, O.; Kubota, Y.; Kondo, J. N.; Okubo, T.; Tatsumi, T. *Stud. Surf. Sci. Catal.* **2007**, *170B*, 1774.

(20) Yokoi, T.; Wakabayashi, J.; Otsuka, Y.; Fan, W.; Iwama, M.; Watanabe, R.; Aramaki, K.; Shimojima, A.; Tatsumi, T.; Okubo, T. *Chem. Mater.* **2009**, *21*, 3719–3729.

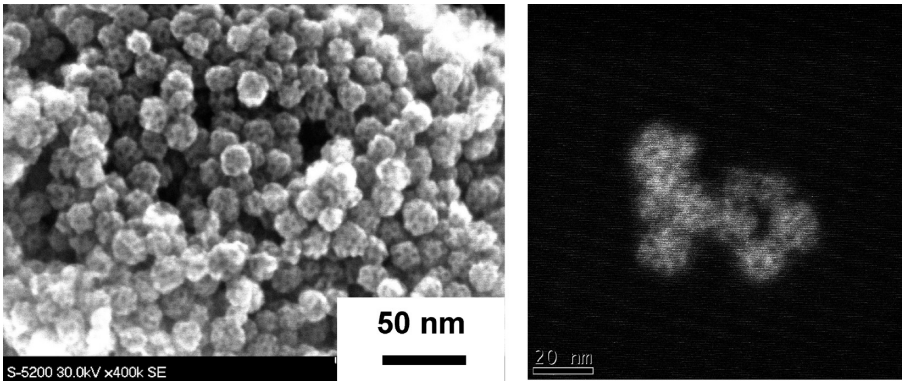

Figure 1. Typical FE-SEM and TEM images of the product after calcination, mesoporous silica nanospheres (MSNSs).

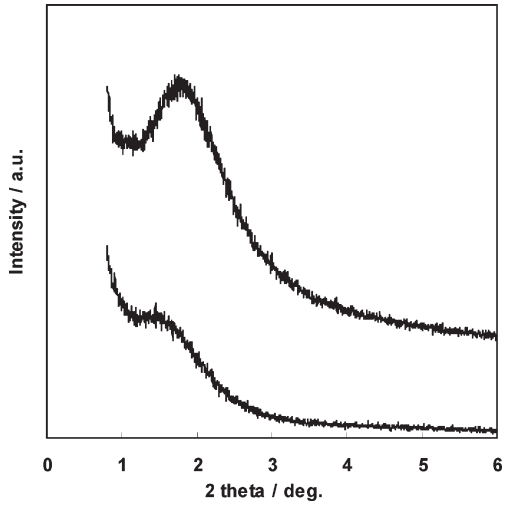

Figure 2. XRD pattern of (a) as-synthesized and (b) calcined products.

condensation of silica networks. In the calcined product, the broad peak is more clearly observed, indicating the formation of uniform-sized mesopores. ^{29}Si MAS NMR measurements indicate that the calcination enhances the condensation of silicate species (see Figure S1 in the Supporting Information).

The nitrogen adsorption−desorption isotherms of the products before and after calcination are shown in Figure 3a. The BET surface area of the as-synthesized product, which was a composite of 58 wt % of silica and 42 wt % of organic components, is found to be 87 $m^2 g^{-1}$. This would be mainly attributed to external surface area of the spheres because mesopores in the spheres were filled with the surfactant molecules. By calcination, the A_{BET} is significantly increased to 585 $m^2 g^{-1}$. Total pore volume (V_p) of the calcined product is found to be 1.4 $cm^3 g^{-1}$.

FE-SEM and TEM observations strongly suggest the presence of uniform mesopores. No capillary condensation step due to the presence of uniform-sized mesopores is observed around $0.3 < P/P_0 < 0.5$ in the isotherms of the product after calcination (Figure 3a). Meanwhile, the pore size (D_p) distribution estimated by the BJH method reveals the presence of uniform pores 2.7 nm in diameter (Figure 3b). Note that there are also pores whose size is broadly distributed between 15 and 25 nm (Figure 3 b), which is likely due to the interparticle voids of MSNSs.

3.2. Role of Basic Amino Acids and Formation Mechanism of MSNSs. The MSNSs were synthesized under weakly basic conditions derived from the basic amino acids; the initial pH in the water phase containing arginine of our synthesis system was 9.7. The synthesis system was changed to weakly acidic conditions (pH 6−7) through the synthesis process.

Usually, the hydrolysis reaction of TEOS for synthesizing the M41S type mesoporous silicas is conducted under much more basic conditions (pH 12−13),[1] Furthermore, the condensation reaction of silicate species leads to the increase in pH because of the production of OH^- ($\equiv Si-O^- + HO-Si\equiv \rightarrow \equiv Si-O-Si\equiv + OH^-$) under basic conditions.[21] In contrast, a slight change in the pH for the opposite direction was observed in our system. This is probably due to consumption of OH^- species ($\equiv Si-OH + HO^- \rightarrow \equiv Si-O^- + H_2O$) as well as the formation of a large number of weakly acidic silanol groups (see Figure S1 in the Supporting Information). The presence of arginine with a buffering action might cause the slight reduction in the pH during the synthesis as well as a weak base catalyst to achieve a slow hydrolysis of TEOS. Huo et al. also reported that a certain acid−base buffer capacity of the reaction mixture in a range of pH 6−10 is essential for the formation of mesoporous silica nanoparticles in the TEOS-cetyltrimethylammonium cation (CTA^+) system.[18]

In the ^{13}C CP/MAS NMR spectrum of the as-synthesized product, two peaks are observed at 158 and 54 ppm in addition to the peaks attributed to C_{16}TMACl (see Figure S2 in the Supporting Information). These peaks are attributed to C atoms in the guanidine group ($H_2NC(=NH)NH-$) and the amino group ($-C(NH_2)(COOH)$) of arginine, indicating that arginine is present in the as-synthesized product.[22] A part of the arginine molecules would be located at the interface between the surfactant micelle and silica wall and/or the external surface of MSNSs during the synthesis process because the arginine molecules can electrostatically interact with both cationic surfactants and anionic silicates.

(21) (a) Iler,R. K. *The Chemistry of Silica*; Wiley: New York, 1978., (b) Brinker, C. J.; Scherer, G. W. *Sol−Gel Science*; Elsevier: Amsterdam, 1990.
(22) Silverstein, R. M.; Webster, F. X. *Spectrometric Identification of Organic Compunnds*, 6th ed.; John Wiley & Sons: New York, 1999.

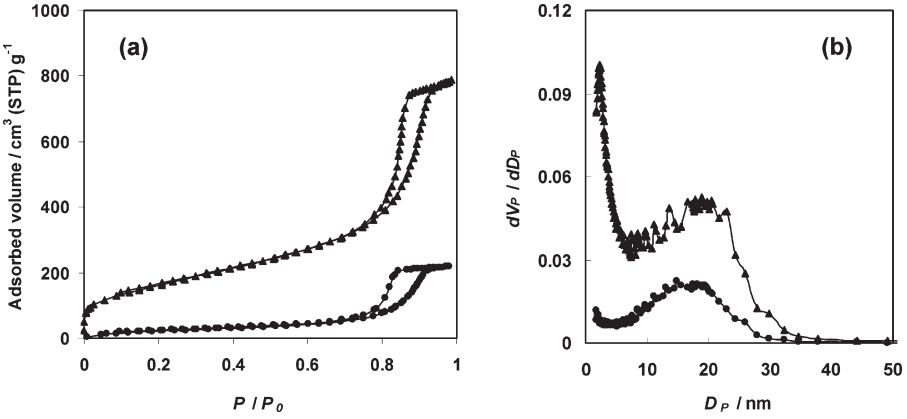

Figure 3. (a) Nitrogen adsorption−desorption isotherms of the products before and after calcination and (b) corresponding pore size distribution by the BJH method using adsorption branch. (D_P, pore diameter; V_P, pore volume).

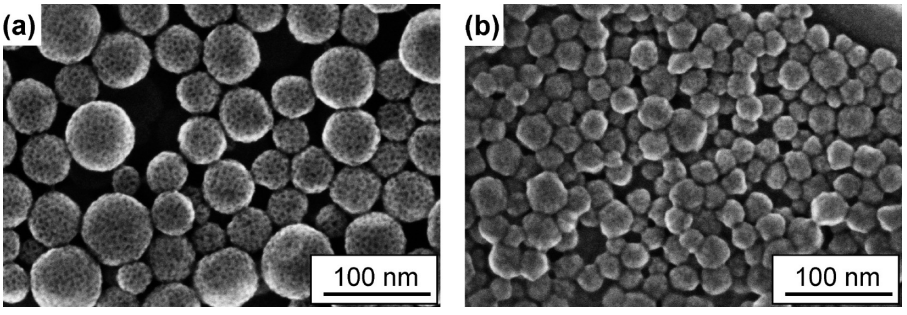

Figure 4. Representative SEM images of the product synthesized with (a) NH_3 or (b) n-$C_3H_7NH_2$ in place of arginine (molar composition 1:0.13:0.12:2000 TEOS:C_{16}TMACl:NH_3 or n-$C_3H_7NH_2$:H_2O).

In addition to arginine, lysine and histidine are categorized into basic amino acids. The use of lysine led to the formation of MSNSs similar to those prepared by using arginine. However, the use of histidine under the same conditions was unsuccessful, possibly because of its relatively low basicity.

As a control, the use of ammonia and *n*-propylamine in place of arginine was examined; the molar composition of the reactants was 1:0.13:0.04:600 TEOS:C_{16}TMACl:NH_3 or n-$C_3H_7NH_2$:H_2O. In the case of ammonia, mesoporous silica spheres were obtained but their sizes ranged from 20 to 80 nm (Figure 4a). One broad peak at $2\theta = 1.8°$ was observed in the XRD pattern of the calcined product (see Figure S3a in the Supporting Information). By the N_2 adsorption−desorption measurements, the A_{BET} of the product was found to be 426 $m^2\ g^{-1}$ (see Figure S3b in the Supporting Information). In the cases of *n*-propylamine, no marked diffraction peak attributed to the formation of mesostructure was observed (see Figure S4a in the Supporting Information). The product was aggregated silica particles 20−50 nm in size and the presence of intraparticle pores was not confirmed (Figure 4b), and the A_{BET} was found to be 183 $m^2\ g^{-1}$ (see Figure S4b in the Supporting Information), indicating that the construction of uniform-sized mesopores in the silica particles was not attained. Hence, weakly basic conditions derived from the basic amino acids are indispensable for the formation of MSNSs.

As a control, TEOS was reacted in the solution containing Arg in the absence of C_{16}TMACl; the mixture containing TEOS, Arg, and H_2O with the molar composition of 1:0.04:600 TEOS:Arg:H_2O was stirred at 333 K for 24 h (this synthesis process is similar to that for the preparation of silica nanospheres (SNSs) though the molar composition of the reactants was different). The resultant product was only aggregates of nonporous silica particles 10−20 nm in size (see Figure S5 in the Supporting Information).

In general, the M41S-type mesoporous silicas are synthesized by using a cationic surfactant and TEOS under strongly basic conditions,[23] leading to fast hydrolysis of TEOS to produce silicate species. Formation of mesostructured silica depends upon surfactant micelles as a template for the assembly and subsequent and/or simultaneous condensation of silicate species.[24] In contrast, in our synthesis system of MSNSs, the hydrolysis of TEOS is quite slow because of relatively low pH and the emulsion system, but the condensation reaction easily occurs.[21] The produced silicate species were consumed for condensation followed by nucleation, forming amorphous silica particles, and electrostatically interacted with the cationic surfactant, forming the silica−micelle composite. The continuous growth and assembly of both the silica particle and the silica−micelle composite, however, might be

(23) Kresge, C. T.; Leonowicz, M. E.; Roth, W. J.; Vartuli, J. C.; Beck, J. S. *Nature* **1992**, *359*, 710–712.
(24) (a) Schacht, S.; Huo, Q.; Voigt-Martin, I. G.; Stucky, G. D.; Schüth, F. *Science* **1996**, *273*, 768–771. (b) Huo, Q.; Feng, J.; Schuth, F.; Stucky, G. D. *Chem. Mater.* **1997**, *9*, 14–17.

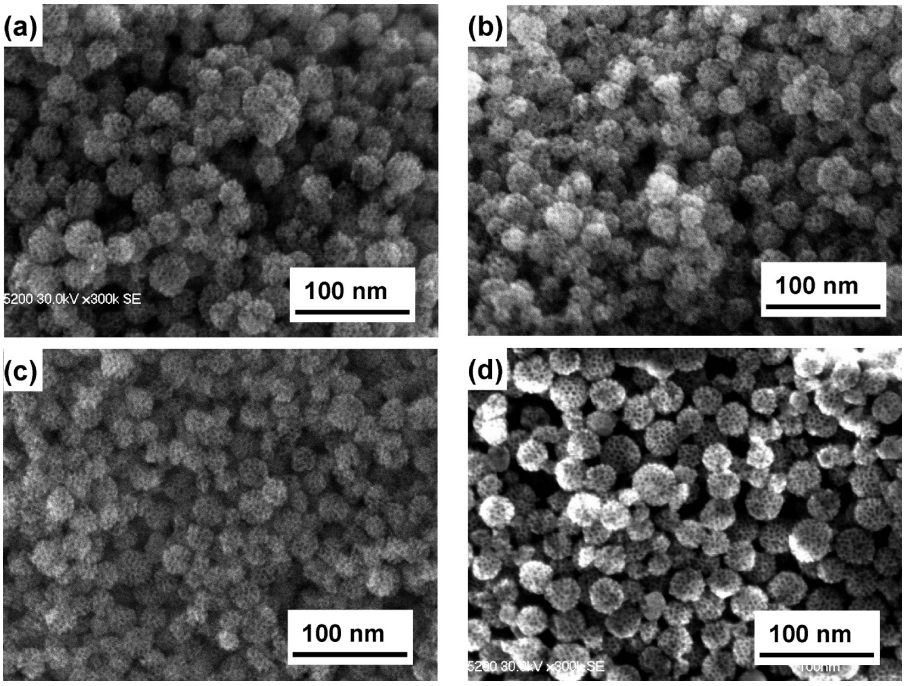

Figure 5. FE-SEM images of the products synthesized with the composition of Arg varied. The molar composition of the reactants was 1:0.13:*x*:2000 TEOS: C_{16}TMACl: Arg: H_2O, where x = (a) 0.04, (b) 0.06, (c) 0.08, and (d) 0.12.

restricted because of the low concentration of silicates species. Because reactive silanol groups are present on the surface of the silica particles,[20] the silica−micelle composite might adhere to the amorphous silica particles through the electrostatic interaction and/or the condensation reaction, leading to the formation of MSNSs with a unique pore structure.

3.3. Effects of Amount of the Reactants on the Morphology and Porosity of MSNSs. *3.3.1. Basic Amino Acid.* The MSNSs were synthesized under the stirring rate of 600 rpm with the molar composition of arginine varied; the molar composition of the reactants was 1:0.13:*x*:2000 TEOS:C_{16}TMACl:Arg:H_2O, where x was the molar composition of Arg. As a control, no silica product was obtained at $x = 0$, likely because of the lack of catalysis for the hydrolysis of TEOS followed by condensation of the resultant products. The representative FE-SEM images of the products with the composition of arginine varied are shown in Figure 5. When x was increased from 0.04 to 0.12, the morphology of the resultant products was practically the same regardless of x; spherical MSNSs 20−30 nm in size were obtained. It was found, however, that the intensity of the main peak of the XRD pattern was increased and its position was slightly shifted to a higher angle (Figure 6a) and that in the nitrogen adsorption−desorption isotherms (Figure 6b), a capillary condensation step became gradually noticeable at a relative pressure of 0.3−0.4 along with increasing x. The BET surface area and total pore volume were simultaneously increased; the A_{BET} and V_p at $x = 0.12$ were ca. 851 $m^2\ g^{-1}$.and 1.8 $cm^3\ g^{-1}$, respectively. These results imply that the pore structure is changed; a craterlike pore would be developed into a typical cylindrical pore; the MSNSs obtained at $x = 0.12$ have cylindrical intraparticle pores 3.0 nm in diameter, which was based on the BJH pore size distribution as well as STEM images (see Figure S6 in the Supporting Information). The increase in arginine as a base led to the slight increase in the pH in the starting solution; when x was 0.04 and 0.12, the pH was found to be 9.7 and 10.2, respectively. It is known that the rate of hydrolysis of TEOS, condensation of silicate species and the solubility of silicate species are drastically changed at the boundary between pH 9 and 10.[21] A slight increase in the pH thus strongly enhances the hydrolysis rate, producing more silicate species at the initial stage of the reaction. Such conditions can increase the local concentration of the micelles by being surrounded with thus produced silicate species. Consequently, the spherical-shaped silica-micelles composites might be transformed into cylindrical-shaped ones, leading to the change in pores structure.

3.3.2. Water. The MSNSs were synthesized with the molar composition of water varied; the molar composition of the reactants was 1 TEOS: 0.13 C_{16}TMACl: 0.12 Arg: y H_2O, where y ranged from 2000 to 6000. The particle size was increased and the size uniformity declined with an increase in y; the mean size of the product at y = 6000 was found to be 200 nm (Figure7). The porosity of the products were almost unchanged; the A_{BET}, D_p and V_p at $y = 6000$ were ca. 838 $m^2 \cdot g^{-1}$, 2.8 nm and 1.1 $cm^3 \cdot g^{-1}$, respectively. Marked changes in the XRD patterns of the products were not observed (Figure S7). These results suggest that the particles size can be tuned by changing the amount of water with the porosity kept.

The increase in the amount of water led to the slight decrease in the pH in the starting solution; the pH values at $y = 3000$ and 6000 were found to be 10.7 and 10.5, respectively. As described above, this slight decrease in the

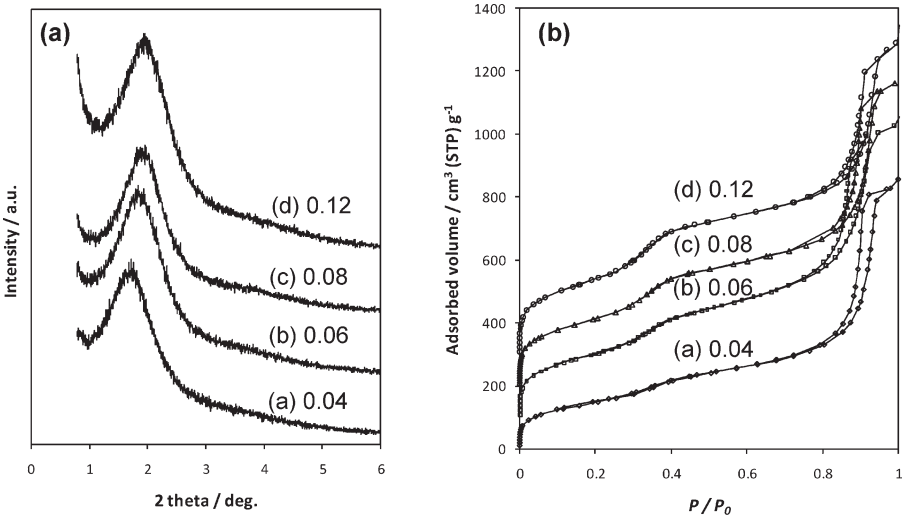

Figure 6. (a) XRD patterns and (b) nitrogen adsorption−desorption isotherms of the products synthesized with the composition of Arg varied. The molar composition of the reactants was 1:0.13:*x*:2000 TEOS:C_{16}TMACl:Arg:H_2O, where x = (a) 0.04, (b) 0.06, (c) 0.08, and (d) 0.12.

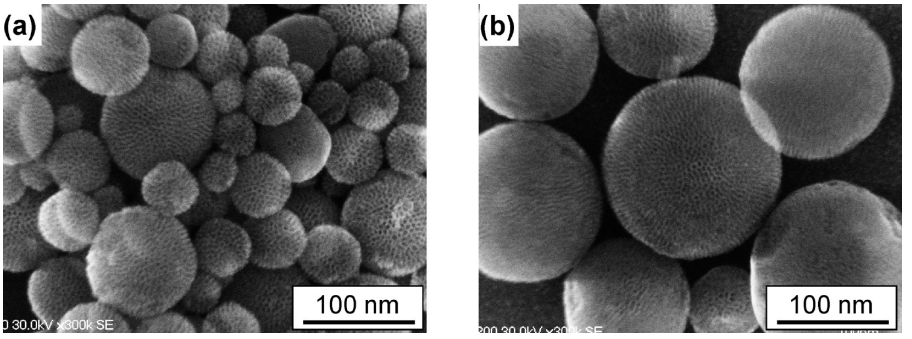

Figure 7. FE-SEM images of the products synthesized with the composition of water varied. The molar composition of the reactants was 1:0.13:0.12:*y* TEOS:C_{16}TMACl:Arg:H_2O, where y = (a) 3000 and (b) 6000.

pH would retard the hydrolysis of TEOS followed by the production of anionic silicates. The number of nuclei of MSNSs would be decreased and the growth of the silica−micelle composite would be enhanced under such conditions. The slowly supplied silicate species would interact with the cationic surfactant, without being consumed for the formation of nonporous silica particles. As a result, the particle size would increase with the porosity being maintained.

3.3.3. Surfactant. Finally, the effect of the amount of the surfactant was investigated; the molar composition of the reactants was 1:*z*:0.12:2000 TEOS:C_{16}TMACl:Arg:H_2O, where z ranged from 0.043 to 0.13. The XRD patterns of the products indicate that the intensity of the main peak was slightly decreased with a decrease in z (see Figure S8 in the Supporting Information). The FE-SEM images of the products at $z = 0.086$ and 0.043 are shown in images a and b in Figure 8, respectively, indicating that the particle size was increased with a decrease in z. Note that pores are not clearly observed in each spherical particle of the product at $z = 0.043$ (Figure 8b). In fact, the porosity was decreased with a decease in the amount of the surfactant; the A_{BET} of the products at $z = 0.086$ and 0.043 was found to be 784 and 427 $m^2\ g^{-1}$, respectively, and the V_p was found to be 1.2 and 0.5 $cm^3\ g^{-1}$, respectively. Probably the silicate species would be mainly consumed for the formation of nonporous amorphous silica particles, not for the formation of the silica−micelle composite because of the lack of the surfactant.

3.4. Size Controls of Intraparticle Mesopores and Spheres of MSNSs. The effect of the alkyl chain length of cationic surfactants on the size of intraparticle mesopore was investigated; $C_nH_{2n+1}N^+Me_3Cl^-$ (n = 10, 12, 14, 16, and 18) was used as a surfactant, and the molar composition of the reactants was 1:0.13:0.12:2000 TEOS:C_nTMACl:Arg:H_2O. The products obtained at $n = 10$ and 12 were not MSNSs; FE-SEM indicated that the products had morphology of irregular shaped particles 200−300 nm in size and their XRD exhibited no diffraction peak at $2\theta = 1-3°$. The products obtained at $n = 14$ and 18 were spherical particles 20−40 nm in size like the product at $n = 16$. One broad peak was observed in the XRD patterns of these products, indicating the presence of uniform-sized mesopores with a low regularity. Note that its peak position was shifted to a lower angle with an increase in the alkyl chain length; 2θ is 2.2, 1.8, and 1.6° at $n = 14$, 16, and 18, respectively (see Figure S9a in the Supporting Inforamtion). The corresponding pore size distributions indicates that the pore size was varied from 2.2 to 3.2 nm depending on the alkyl chain length of

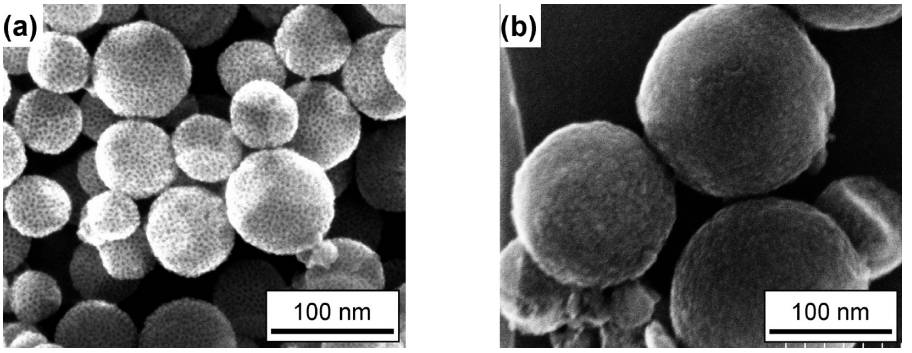

Figure 8. FE-SEM images of the products synthesized with the composition of the surfactant varied. The molar composition of the reactants was 1:z:0.12:2000 TEOS:C_{16}TMACl:Arg:H_2O, where z = (a) 0.086 and (b) 0.043.

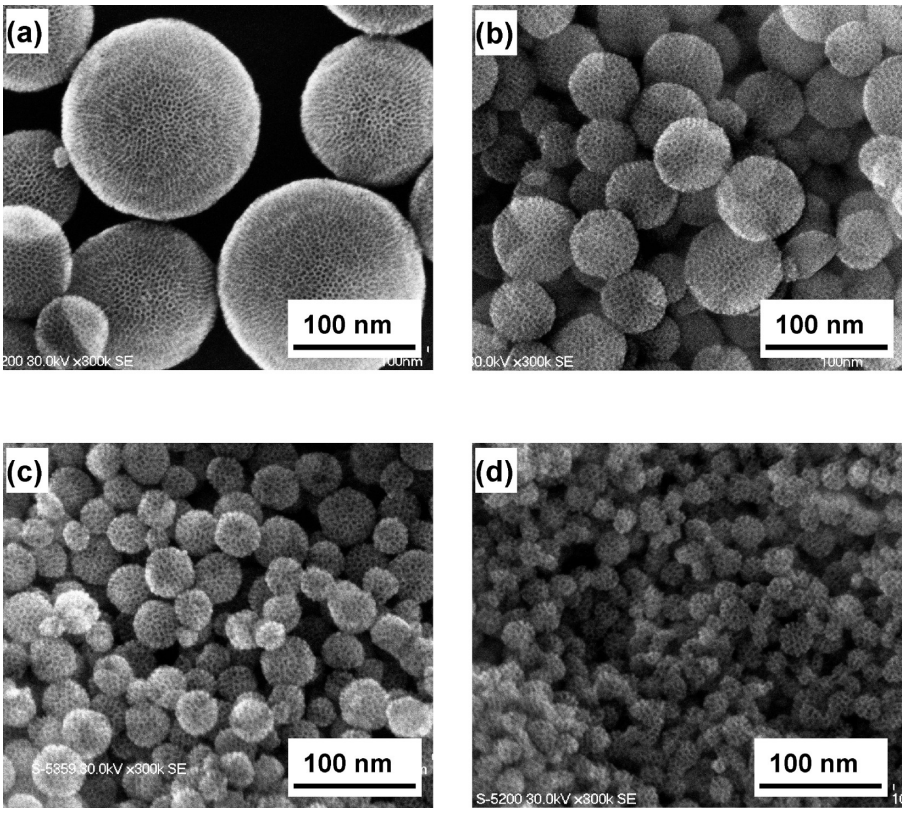

Figure 9. FE-SEM images of the MSNSs products with the stirring rate varied: (a) 0, (b) 300, (c) 450, and (d) 600 rpm. The mother gel composition was 1:0.13:0.12:2000 TEOS:C_{16}TMACl:Arg:H_2O.

cationic surfactants (see Figure S9b in the Supporting Information).

The size of spheres can be regulated in the range of 15−200 nm by varying the molar compositions of the reactants (e.g., surfactant and water). Moreover, the size has been found to be drastically sensitive to the stirring rate of the synthesis system after addition of TEOS. The FE-SEM images of the products synthesized with the stirring rate varied ranging from 0 to 600 rpm indicate that the size of spheres are decreased with an increase in the stirring rate and that the size uniformity is simultaneously raised (Figure 9); e.g., the mean sizes of MSNSs are estimated to be 150 and 25 nm at the stirring rate of 0 and 600 rpm, respectively. In contrast, when the stirring rate was further increased, the morphology of the resultant product was unchanged. The fast stirring enhances the hydrolysis rate of TEOS, leading to the formation of more silica particles at the initial stage of the reaction. Consequently, the smaller-sized MSNSs were obtained. On the other hand, the slow stirring retards the hydrolysis of TEOS in the emulsion system. Based on the Ostwald ripening process,[25] the produced silicate species are preferably consumed for the growth of preformed amorphous silica particles and the silica−micelle composite, resulting in the formation of larger-sized SNSs with a low yield based on the TEOS used. Moreover, the growth of the preformed particles under the static conditions

(25) Gao, G. *Nanostructures & Nanomaterials*; Imperial College Press: London, 2004.

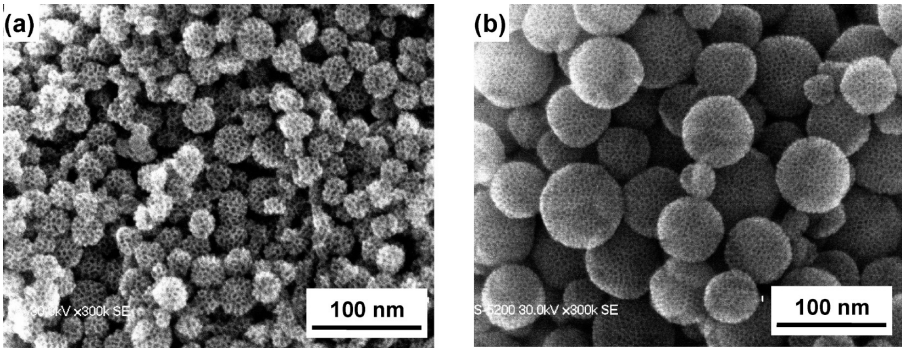

Figure 10. FE-SEM images of the Ti-MSNSs averaging (a) 25 and (b) 70 nm in size.

would heterogeneously proceed, resulting in the formation of different-sized MSNSs.

3.5. Preparation of Ti-Containing MSNSs and Their Catalytic Performances. Tetrahedrally coordinated Ti-containing mesoporous silica has been used as a heterogeneous catalyst for selective oxidation of bulky organic compounds. For the purpose of enhancing oxidation capabilities, the introduction of Ti onto the wall of MSNSs was examined. Attempts to synthesize Ti-MSNSs via a direct route, which is based on the addition of TBOT into the starting solution, were unsuccessful; although the MSNSs were obtained, the octahedrally coordinated Ti species and the anatase-like ones were predominant in the product.

A post-treatment method based on the introduction of a Ti precursor into the MSNSs was adopted to prepare Ti-MSNSs. In this method, TBOT in the EtOH solution was slowly treated with H_2O_2, forming Ti peroxo-complex, a stable titanium source. Thus formed Ti precursors were allowed to react with silanol groups on the extracted MSNSs. Two kinds of different-particle-sized Ti-MSNSs were prepared by using 25 and 70 nm average-sized MSNSs having cylindrical intraparticle pores about 3 nm in diameter. From the ICP analysis, their Si/Ti atomic ratios in the final products were estimated to be 98 and 84, respectively. Figure 10 shows the FE-SEM images of the calcined Ti-MSNSs samples, revealing that the morphology of Ti-MSNSs was retained after the post-treatment. It was also confirmed by XRD and the nitrogen adsorption−desorption measurements that the mesostructure and the porosity were also retained. The A_{BET} of Ti-MSNSs of 25 and 70 nm average size were ca. 820 and 835 $m^2\ g^{-1}$, respectively. Figure 11 shows the diffuse reflectance UV−vis spectra of the Ti-MSNSs, indicating that a single peak at 220 nm is mainly observed. In conclusion, tetrahedrally coordinated Ti species are successfully introduced onto the MSNSs regardless of the size of spheres.

Finally, the catalytic performance of thus prepared Ti-MSNSs in epoxidation of different-sized alkenes, cyclohexene, *cis*-stilbene and caryophyllene, using TBHP as an oxidant was examined. As a control, 1−2 μm sized Ti-MCM-41 (Si/Ti = 88 and A_{BET} = 1013 $m^2\ g^{-1}$), which

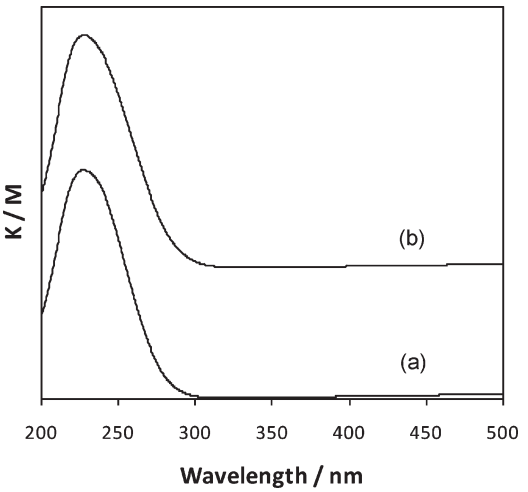

Figure 11. UV−vis. spectra of (a) Ti-MSNSs *av*. 25 nm (Si/Ti = 98) and (b) Ti-MSNSs *av*. 70 nm (Si/Ti = 84).

was prepared according to the literature with modifications,[26] was also evaluated. The conversion of the substrate and the yield of the desired epoxide product are plotted against the reaction time (Figure 12). Ti-MCM-41 exhibited the highest catalytic activity in the epoxidation of cyclohexene. On the other hand, the catalytic activities of Ti-MSNSs of 25 nm average size for the epoxidation of the more bulky alkenes, *cis*-stilbene and caryophyllene, were higher than those of either Ti-MSNSs of 70 nm average size or Ti-MCM-41. These results are in agreement with our expectation that small particle size is beneficial to mass transport of bulky molecules. Although the interparticle voids of mesoporous silica nanoparticles have been used as a catalyst support to facilitate easier transport,[27−30] the influences of the sizes of particle and interparticle void on the catalytic performance have not fully been investigated. In our cases, the unique pore structure consisting of intraparticle pores of about 3 nm and interparticle large mesopores of about

(26) Igarashi, N.; Kidani, S.; Ahemaito, R.; Hashimoto, K.; Tatsumi, T. *Microporous Mesoporous Mater*. **2005**, *81*, 97–105.
(27) Fotopoulos, A. P.; Triantafyllidis, K. S. *Catal. Today* **2007**, *127*, 148–156.
(28) Ortiz de Zarate, D.; Gomez-Moratalla, A.; Guillem, C.; Beltran, A.; Latorre, J.; Beltran, D.; Amoros, P. *Eur. J. Inorg. Chem*. **2006**, *13*, 2572–2581.
(29) Pauly, T. R.; Liu, Y.; Pinnavaia, T. J.; Billinge, S. J. L.; Rieker, T. P. *J. Am. Chem. Soc*. **1999**, *121*, 8835–8842.
(30) Prouzet, E.; Cot, F.; Nabias, G.; Larbot, A.; Kooyman, P.; Pinnavaia, T. J. *Chem. Mater*. **1999**, *11*, 1498–1503.

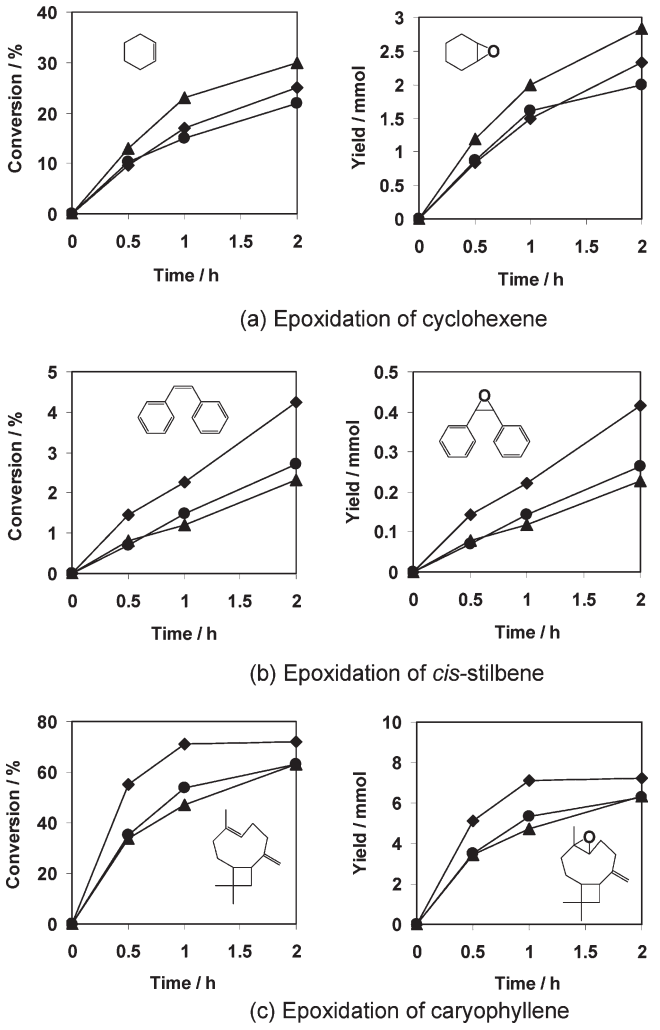

Figure 12. Epoxidation of cyclohexene, *cis*-stilbene, and caryophyllene using TBHP as an oxidant over Ti-MSNSs and Ti-MCM-41. Reaction conditions: Cat., 25 mg; cyclohexene, 10 mmol; TBHP, 10 mmol; temperature, 303 K. ♦Ti-MSNSs averaging 25 nm (Si/Ti = 98), ●Ti-MSNSs averaging 70 nm (Si/Ti = 84), ▲ Ti-MCM-41 (Si/Ti = 88).

20 nm has proved to be advantageous to the liquid phase epoxidation of bulky alkenes.

4. Conclusions

The average 20 nm sized mesoporous silica nanospheres (MSNSs) having cratelike mesopores about 3 nm in diameter have been successfully synthesized. Assembly of MSNSs resulted in the formation of interparticle voids. The size of the discrete spheres can be regulated in the range of 15−200 nm by, for example, changing the stirring rate in the synthesis stage. Tetrahedrally coordinated Ti containing MSNSs (Ti-MSNSs) were also prepared by a post-treatment method. Ti-MSNSs of small size exhibited a high catalytic performance in the epoxidation of bulky alkenes, *cis*-stilbene and caryophyllene. Thus obtained mesoporous silica nanospheres with a unique pore structure in the controlled morphology will be also advantageous to general applications in catalysis and adsorption host−guest chemistry in terms of efficient mass transport of guest molecules, and they also have a potential for biomedical applications.[31−37]

Acknowledgment. We thank Prof. Osamu Terasaki and Dr. Yasuhiro Sakamoto (Stockholm University) for the structural characterizations. This work was supported by Grant-in-Aid for Scientific Research (S) (19106015) of Education, Culture, Sports, Science and Technology of Japan (MEXT). This work was also partly supported by Research and Development in a New Interdisciplinary Field Based on Nanotechnology and Materials Science Program of the Ministry of MEXT.

Supporting Information Available: ^{29}Si MAS and ^{13}C CP/MAS NMR spectra, XRD patterns, nitrogen sorption isotherms, pore size distributions and FE-SEM and STEM images of the prepared samples. This material is available free of charge via the Internet at http://pubs.acs.org.

(31) Fadeel, B.; G.-B. Alfonso, E. *Adv. Drug Delivery Rev.* **2010**, *62*, 362–374.
(32) Vivero-Escoto, J. L.; Slowing, I. I.; Lin, V. S.-Y. *Biomaterials* **2010**, *31*, 1325–1333.
(33) Huang, X.; Teng, X.; Chen, D.; Tang, F.; He, J. *Biomaterials* **2010**, *31*, 438–448.
(34) Li, X.; Hong, C.-Y.; Pan, C.-Y. *Polymer* **2010**, *51*, 92–99.
(35) Lin, Y.-S.; Haynes, C. L. *Chem. Mater.* **2009**, *21*, 3979–3986.
(36) Klichko, Y.; Liong, M.; Choi, E.; Angelos, S.; Nel, A. E.; Stoddart, J. F.; Tamanoi, F.; Zink, J. I. *J. Am. Ceram. Soc.* **2008**, *92*, S2–S10.
(37) Slowing, I. I.; Vivero-Escoto, J. L.; Wu, C.-W.; Lin, V. S.-Y. *Adv. Drug Delivery Rev.* **2008**, *60*, 1278–1288.